Journal of Beijing Institute of Technology, 2021, Vol. 30, Suppl.1

Conjugate Meshing Analysis of Nutation Drive with Face Gears

Guangxin Wang, Lili Zhu✉, Jiaqi Yue and Yuting Shen
(School of Mechanical Engineering, Dalian Jiaotong University, Dalian 116028, China)

Abstract: A calculation formula of boundary size is proposed to analyze the conjugate meshing of nutation face gear transmission by using the condition of no tip change and root undercutting. Furthermore, the influence of tooth shape design parameters on the boundary dimension of nutation face gears is studied. Based on the meshing principle of spacial gears, the conjugate conditions of the "face-face" gear pair are derived, the calculation method of discrete points of tooth surface is given, and the three-dimensional model of the nutation face gear transmission device is also established, which helps the design and manufacturing of high-quality nutation face gear transmissions and improves its transmission performance.

Key words: conjugate condition; face gear; meshing analysis; nutation drive
CLC number: TH132.4 **Document code:** A **Article ID:** 1004-0579(2021)S1-0064-11

Nutation face gear transmission is a new type of transmission based on the "face-face" gear pair. It replaces the spur gear with an internal face gear to form a "face-face" meshing gear pair, and actualizes its deceleration function by combining the nutation principle, which has the advantages of both face gears and nutation drives, including a large transmission ratio, large coincidence, small size, compact structure, and strong bearing capacity. Compared with a traditional gear reducer, under the same transmission ratio, the nutation face gear reducer needs fewer parts, which is conducive to reducing the manufacturing cost and improving the reliability of the device. It can be widely used in shield machines, helicopter main reducers and other high-power fields, offering high reliability, strong bearing capacity, and a compact structure. As shown in Fig. 1[1-2], the teeth on the fixed face gear labeled 7 and the teeth on the left side of the planetary face gear labeled 24 constitute the "face-face" meshing pair, while the teeth on the right side of the planetary face gear labeled 24 and the teeth on the rotary face gear labeled 23 form another "face-face" meshing pair. When the input shaft labeled 1 rotates at a constant angular speed, it drives the planetary wheel to move the nutation drive. Under the action of the "face-face" gear pairs on both sides, the planetary wheel transfers the motion and torque to the rotary face gear, thus actualizing the deceleration drive.

Research on nutation face gear transmissions is still in its infancy. At present, the tooth surface equation of internal face gears and the meshing equation of "face-face" gear pairs have been derived in detail[2-3]. The single-tooth stiffness, single-tooth time-varying meshing stiffness, and comprehensive meshing stiffness of the internal and external face gears have also been obtained by the simplified trapezoidal section method[4]. However, the structure of nutation face gears still has the characteristics of dedendum

Received 2020-08-03
Supported by the National Natural Science Foundation of China (50905021); the Doctoral Start-up Foundation of Liaoning Province (201601263); the Natural Fund Guidance Scheme of Liaoning Province (20180551106); the Education Department's Scientific Research Funding Project of Liaoning Province (JDL2019010)
✉ Author for correspondence, associate professor, Ph.D.
E-mail: xiaozhuzhu_1979@163.com
DOI: 10.15918/j.jbit1004-0579.20102

undercutting and addendum pointing, and the existing heat treatment technology of gears will cause problems including large thermal deformation of the teeth and inconsistent depth of the hardened layer of tooth surfaces, which will affect the accuracy and strength of the tooth surfaces of nutation face gears. It is necessary to study the conjugate meshing analysis of nutation drives with face gears, so as to obtain the calculation formula of boundary dimensions, derive the conjugate meshing conditions, understand the influence of tooth shape design parameters on boundary dimension and tooth width, and finally, design and manufacture a high-quality nutation face gear transmission.

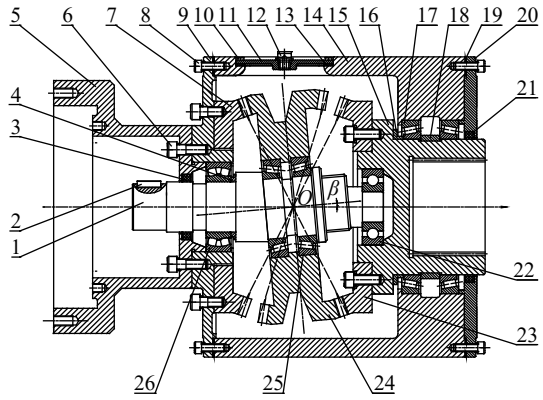

1-Input shaft; 2-Key; 3-Sealing ring; 4-Axle sleeve; 5-Bearing cap; 6-Inside hexagonal bolt; 7-Fixed face gears; 8-Inside hexagonal bolt; 9-Box cover; 10-Hexagonal head bolt; 11-Inspection cover; 12-Breather plug; 13-Inspection hole gasket; 14-Box; 15-Output shaft; 16-Oil baffle; 17-Conical roller bearing; 18-Bearing shoulder; 19-Adjustment washer; 20-Bearing cap; 21-Sealing ring; 22-Deep groove ball bearing; 23-Rotary face gear; 24-Planetary face gear; 25-Conical roller bearing; 26-Spherical roller bearing

Fig. 1 Structural sketch of the nutation face gear transmission device

In 1949, Buckingham[5] first put forward the concept of face gears in his works. He proposed that face gear teeth should be regarded as a rack with variable pressure angle and pitch and that the meshing between a cylindrical gear and a bevel gear should be regarded as the meshing between a cylindrical gear and a rack on different shaft sections. He also obtained the approximate tooth profile of a face gear on different shaft sections through the method of projection geometry. The research of Litvin and his team[6-11] greatly promoted the application of face gears. They used differential geometry and meshing principles to deduce the tooth surface equation of face gears, and obtained the boundary conditions of undercutting and sharpening of face gears. In terms of improving the transmission performance of face gears, Litvin proposed a structure of asymmetric face gear transmission. Claudio et al.[12] proposed the drum shape modification technology of spur gears and studied the meshing performance of face gears through computer simulations, which laid a theoretical foundation for the design of face gear profiles. Zhu et al.[13-17] studied the meshing performance of face gear transmission, put forward a design method to avoid undercutting and tip changing in the face gear design, visualized the contact path of tooth surfaces by using computer simulation technology, and analyzed the influence of load conditions and various installation errors on the meshing and strength performance of face gear transmission, which laid a theoretical foundation for further research in China. Zschippang et al.[18] presented a general method for generation of face-gears with helix angle, shaft angle, and axle offset elaborated based on the simulation of the enveloping process of an involute shaper with the face-gear, and discussed the resulting impact on the location of the contact path for meshing of a pinion with the face-gear. Zhu et al.[19] established a piecewise torsional-bending-pendular nonlinear dynamics model of a face-gear drive system to study its nonlinear dynamics and dynamic characteristics, considering multi-state engagements including drive-side teeth engaging, teeth disengagement, back-side teeth engaging, and alternate engaging between single-teeth pair and double-teeth pairs caused by the couple of the backlash and the contact ratio being greater than 1.0.

In the new nutation drive with face gears,

the conjugate pair does not mesh the cylindrical gear and the face gear to actualize the transmission of motion and power; instead, the conjugate "internal" face gear meshes with the face gear to form a new conjugate pair. Although domestic and foreign scholars have made some progress in the research of nutation face gears, the pointing phenomenon of face gears limits the practical application of nutation face gear transmissions. The pointing of the face gear teeth means that the thickness of one end at the top of the tooth is 0. Therefore, the tooth length of a face gear is limited and the bearing capacity of the gear is affected. Because of the nutation angle, this situation also exists and is more prominent in nutation face gear transmissions. Therefore, the aim of this paper is to analyze and deduce the boundary dimension of nutation face gears in a unified coordinate system, and study the influence of tooth shape design parameters on the boundary size and tooth width, which provides a theoretical basis for reasonable selection of parameters. Furthermore, the condition of conjugate meshing of nutation face gears is derived, the generation method of discrete data point coordinates of tooth surfaces is studied, and a three-dimensional model of a nutation face gear transmission device is also established, which helps in the design and manufacturing of a high-quality nutation face gear transmission and improves its transmission performance.

1 Boundary Dimension Analysis of the Nutation Face Gear

In the process of machining nutation face gears with a gear shaper, the meshing angle between the gear shaper and the gear to be machined changes with different meshing positions, and the meshing angle gradually decreases over the changes in meshing position along the axial direction of the nutation face gear until it is 0. In the actual cutting process, the closer the meshing position is to the axis of the face gear, the smaller the meshing angle is; and there is a limit meshing point between the gear shaper and the face gear: that is, the meshing angle cannot be equal to zero. When the meshing angle is too small, the conjugate tooth profile of the nutation face gear will be cut off by the transition part of the tooth top of the gear shaper: that is, the root undercutting phenomenon will occur. The farther away from the axis of the nutation face gear, the larger the meshing angle is and the smaller the tooth top thickness is. When reaching a certain position, the tooth top thickness of the nutation face gear is zero, and the tooth top becomes sharp.

The boundary dimension diagram of nutation face gear is shown in Fig. 2, where L_{in} is the radius of the nutation face gear when root undercutting occurs, which is called the minimum internal radius; L_{out} is the radius of the nutation face gear when tip change occurs, which is called the maximum external radius. The maximum internal radius and the minimum external radius should be measured along the direction of the generatrix on the top cone of the nutation face gear, and the difference between the minimum internal radius and the maximum external radius of nutation face gear is called the effective tooth width B, that is

$$B = L_{out} - L_{in} \tag{1}$$

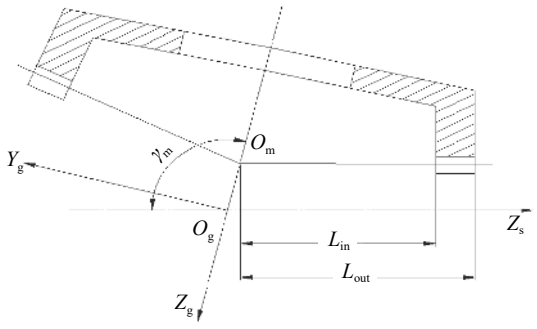

Fig. 2 Boundary dimension of the nutation drive with face gear

1.1 Conditions for no root undercutting

The critical point of undercutting is the intersection of the tooth top circle of the gear

shaper and the limit meshing position of the nutation face gear. The minimum internal radius of the nutation face gear can be obtained by the condition for no root undercutting. At the undercutting critical point on the tooth surface of the shaper tool and the nutation face gear, there is the following relation[11]

$$\boldsymbol{v}^{(\mathrm{s,g})}+\boldsymbol{v}_{\mathrm{s}}=0 \tag{2}$$

where $\boldsymbol{v}_{\mathrm{s}}$ is the absolute velocity of the gear shaper and $\boldsymbol{v}^{(\mathrm{s,g})}$ is the relative velocity of the gear meshing point between the gear shaper and the nutation face gear.

According to the meshing equation of the tooth surface between the shaper cutter and the nutation face gear[2]

$$\begin{aligned}f_{\mathrm{g}}(u_{\mathrm{s}},\theta_{\mathrm{s}},\phi_{\mathrm{s}})=&r_{\mathrm{bs}}(1-m_{\mathrm{s/g}}\cos\gamma_{\mathrm{m}})-\\&u_{\mathrm{s}}m_{\mathrm{s/g}}\sin\gamma_{\mathrm{m}}\cos\phi_{\theta}=0\end{aligned} \tag{3}$$

where θ_{s} is the angle parameter of any point of gear shaper cutter, u_{s} is the axial parameter of a point on the tooth surface of gear shaper, ϕ_{s} is the instantaneous rotation angle of the cutter, r_{bs} is the base circle radius of the cutter, $m_{\mathrm{s/g}}=\dfrac{N_{\mathrm{g}}}{N_{\mathrm{s}}}$ is the tooth ratio of the cutter and the face gear, γ_{m} is the shaft intersection angle between the face gear and the gear shaper, $\phi_{\theta}=\phi_{\mathrm{s}}+\theta_{\mathrm{s}}+\theta_{\mathrm{s0}}$, $\theta_{\mathrm{s0}}=\dfrac{\pi}{2N_{\mathrm{s}}}-\mathrm{inv}\alpha_{\mathrm{s}}$ is the angle parameter from the symmetrical line to the starting point of the involute, α_{s} is the pressure angle of the cutter, and N_{s} and N_{g} represent the teeth number of the gear shaper and the gear on the machined surface, respectively. Taking into account that Eq. (3) is the same for all times t, and differentiating it, the equations needed to determine the existence of the undercutting boundary line on the cutter tooth surface are sorted out, and the results are as follows.

$$\begin{cases}\boldsymbol{r}_{\mathrm{s}}=\boldsymbol{r}_{\mathrm{s}}(\theta_{\mathrm{s}},\phi_{\mathrm{s}})\\ f_{\mathrm{g}}(u_{\mathrm{s}},\theta_{\mathrm{s}},\phi_{\mathrm{s}})=0\\ \dfrac{\partial f_{\mathrm{g}}(u_{\mathrm{s}},\theta_{\mathrm{s}},\phi_{\mathrm{s}})}{\partial t}=0\end{cases} \tag{4}$$

where $\boldsymbol{r}_{\mathrm{s}}$ is the tooth surface vector of the cutter.

By simplifying Eq. (4), we can get

$$\Delta=\begin{vmatrix}\dfrac{\partial x_{\mathrm{s}}}{\partial u_{\mathrm{s}}} & \dfrac{\partial x_{\mathrm{s}}}{\partial \theta_{\mathrm{s}}} & v_{x}^{(\mathrm{s,g})}\\ \dfrac{\partial z_{\mathrm{s}}}{\partial u_{\mathrm{s}}} & \dfrac{\partial z_{\mathrm{s}}}{\partial \theta_{\mathrm{s}}} & v_{z}^{(\mathrm{s,g})}\\ f_{u_{\mathrm{s}}} & f_{\theta_{\mathrm{s}}} & f_{\phi_{\mathrm{s}}}\dfrac{\mathrm{d}\phi_{\mathrm{s}}}{\mathrm{d}t}\end{vmatrix}=0 \tag{5}$$

where x_{s} and z_{s} are the coordinates of any point of the tool on the x and z axes, respectively; $v_{x}^{(\mathrm{s,g})}$ and $v_{z}^{(\mathrm{s,g})}$ are the components of relative velocity $\boldsymbol{v}^{(\mathrm{s,g})}$ on the x and z axes, respectively; $f_{u_{\mathrm{s}}}$, $f_{\theta_{\mathrm{s}}}$ and $f_{\phi_{\mathrm{s}}}$ are the uppartial derivatives of Eq. (3) to u_{s}, θ_{s} and ϕ_{s}, respectively, $f_{u_{\mathrm{s}}}=\dfrac{\partial f_{\mathrm{g}}}{\partial u_{\mathrm{s}}}=-m_{\mathrm{s/g}}\sin\gamma_{\mathrm{m}}\cos\phi_{\theta}$, $f_{\theta_{\mathrm{s}}}=\dfrac{\partial f_{\mathrm{g}}}{\partial \theta_{\mathrm{s}}}=u_{\mathrm{s}}m_{\mathrm{s/g}}\sin\gamma_{\mathrm{m}}\sin\phi_{\theta}$, and $f_{\phi_{\mathrm{s}}}\dfrac{\mathrm{d}\phi_{\mathrm{s}}}{\mathrm{d}t}=\dfrac{\partial f_{\mathrm{g}}}{\partial \phi_{\mathrm{s}}}\dfrac{\mathrm{d}\phi_{\mathrm{s}}}{\mathrm{d}t}=u_{\mathrm{s}}m_{\mathrm{s/g}}\omega_{\mathrm{s}}\sin\gamma_{\mathrm{m}}\sin\phi_{\theta}$.

After arranging Eq. (5), the following equation can be derived

$$\begin{aligned}f_{\mathrm{g}}(u_{\mathrm{s}},\theta_{\mathrm{s}},\phi_{\mathrm{s}})=&\frac{\partial x_{\mathrm{s}}}{\partial u_{\mathrm{s}}}\left(\frac{\partial z_{\mathrm{s}}}{\partial \theta_{\mathrm{s}}}f_{\phi_{\mathrm{s}}}\frac{\mathrm{d}\phi_{\mathrm{s}}}{\mathrm{d}t}-v_{z}^{(\mathrm{s,g})}f_{\theta_{\mathrm{s}}}\right)-\\&\frac{\partial x_{\mathrm{s}}}{\partial \theta_{\mathrm{s}}}\left(\frac{\partial z_{\mathrm{s}}}{\partial u_{\mathrm{s}}}f_{\phi_{\mathrm{s}}}\frac{\mathrm{d}\phi_{\mathrm{s}}}{\mathrm{d}t}-v_{z}^{(\mathrm{s,g})}f_{u_{\mathrm{s}}}\right)+\\&v_{x}^{(\mathrm{s,g})}\left(\frac{\partial z_{\mathrm{s}}}{\partial u_{\mathrm{s}}}f_{\theta_{\mathrm{s}}}-\frac{\partial z_{\mathrm{s}}}{\partial \theta_{\mathrm{s}}}f_{u_{\mathrm{s}}}\right)=0\end{aligned} \tag{6}$$

where $\dfrac{\partial x_{\mathrm{s}}}{\partial u_{\mathrm{s}}}=0$, $\dfrac{\partial z_{\mathrm{s}}}{\partial u_{\mathrm{s}}}=0$, $\dfrac{\partial z_{\mathrm{s}}}{\partial \theta_{\mathrm{s}}}=0$, and $\dfrac{\partial x_{\mathrm{s}}}{\partial \theta_{\mathrm{s}}}=r_{\mathrm{bs}}\theta_{\mathrm{s}}\sin(\theta_{\mathrm{s0}}+\theta_{\mathrm{s}})$.

Using the specific form of the above parameters in Eq. (6) and rearranging it, the following equation can be obtained

$$\begin{aligned}&A\theta_{\mathrm{s}}m_{\mathrm{s/g}}^{2}\sin^{2}\gamma_{\mathrm{m}}\cos^{3}\phi_{\theta}+A(1-m_{\mathrm{s/g}}\cos\gamma_{\mathrm{m}})^{2}\sin\phi_{\theta}+\\&\theta_{\mathrm{s}}(1-m_{\mathrm{s/g}}\cos\gamma_{\mathrm{m}})\sin\phi_{\theta}\cos\phi_{\theta}=0\end{aligned} \tag{7}$$

where $\theta_{\mathrm{s}}=\theta_{\mathrm{s}}^{*}=\sqrt{r_{\mathrm{as}}^{2}-r_{\mathrm{bs}}^{2}}/r_{\mathrm{bs}}$, θ_{s}^{*} is the angle parameter of the tool tooth surface at its tooth top circle, r_{as} is the tooth top circle radius of the cutter, and $A=\sin\phi_{\theta}-\theta_{\mathrm{s}}\cos\phi_{\theta}$.

From Eq. (5), the value of parameter $\phi_{\mathrm{s}}=\phi_{\mathrm{s}}^{*}$ can be obtained. According to the face gear tooth surface equation[2] as

$$\begin{aligned}\boldsymbol{r}_{\mathrm{g}}(\theta_{\mathrm{s}},\phi_{\mathrm{s}})=&\begin{bmatrix}x_{\mathrm{g}}\\ y_{\mathrm{g}}\\ z_{\mathrm{g}}\\ 1\end{bmatrix}=\\&\begin{bmatrix}r_{\mathrm{bs}}(A\cos\phi_{\mathrm{g}}-D\cos\gamma_{\mathrm{m}}\sin\phi_{\mathrm{g}}-C\sin\phi_{\mathrm{g}})\\ -r_{\mathrm{bs}}(A\sin\phi_{\mathrm{g}}+D\cos\gamma_{\mathrm{m}}\cos\phi_{\mathrm{g}}+C\cos\phi_{\mathrm{g}})\\ -r_{\mathrm{bs}}(D\sin\gamma_{\mathrm{m}}-C\cot\gamma_{\mathrm{m}})\\ 1\end{bmatrix}\end{aligned} \tag{8}$$

where $D=\cos\phi_\theta+\theta_s\sin\phi_\theta$, $C=\dfrac{1-m_{s/g}\cos\gamma_m}{m_{s/g}\cos\phi_\theta}$, and $\phi_g=m_{s/g}\phi_s$. By substituting ϕ_s^* and θ_s^* into Eq. (8), $x_g(\theta_s^*,\phi_s^*)$, $y_g(\theta_s^*,\phi_s^*)$ and $z_g(\theta_s^*,\phi_s^*)$ can be obtained. Then, the minimum internal radius L_{in} that does not produce a root undercutting condition of the nutation face gear is derived as

$$L_{in}=\sqrt{x_g^2(\theta_s^*,\phi_s^*)+[-y_g(\theta_s^*,\phi_s^*)\sin\gamma_m+z_g(\theta_s^*,\phi_s^*)\cos\gamma_m+r_{ds}\cot\gamma_m)^2} \tag{9}$$

1.2 Conditions for no tip change

The strength of the teeth will be weakened if the tops of the teeth are tapered, which means that the tooth thickness at the tops of the teeth is equal to zero. When the tip of the nutation face gear becomes sharp, the tooth surfaces on both sides of the tooth intersect, and the tooth top thickness is equal to zero. It is assumed that a cone at the top of the face gear tooth is used to cross the tooth surfaces on both sides of the gear. The cone surface is coaxial with the gear shaper cutter and tangent to a cylinder with radius $r_{ds}=r_{ps}-m_s$, where r_{ps} and m_s are the pitch circle radius and the module of the gear shaper cutter, respectively. It should be noted that when $r_{ds}<r_{bs}$, $r_{ds}=r_{bs}$ should be taken.

According to the symmetry of the tooth surfaces on both sides of the nutation face gear teeth, the cusp changing position of the tooth top should be on the symmetry plane Y_gOZ_g. Then, the coordinates at the cusp changing position meet the following requirements

$$\begin{aligned}&x_g(\theta_s^{**},\phi_s^{**})=0\\&-y_g(\theta_s^{**},\phi_s^{**})\cot\gamma_m+\frac{r_{ds}}{\sin\gamma_m}+z_g(\theta_s^{**},\phi_s^{**})=0\end{aligned} \tag{10}$$

By substituting $x_g(\theta_s^{**},\phi_s^{**})$ and $z_g(\theta_s^{**},\phi_s^{**})$ into Eq. (8), the corresponding parameters θ_s and ϕ_s as θ_s^{**} and ϕ_s^{**} can be obtained, and then θ_s^{**} and ϕ_s^{**} can be substituted into the Eq. (8), and the value of $y_g(\theta_s^{**},\phi_s^{**})$ can be obtained. Therefore, the maximum outer radius L_{out} of the tooth tip of nutation face gear without tip change is

$$L_{out}=-y_g(\theta_s^{**},\phi_s^{**})/\sin\gamma_m \tag{11}$$

2 Influence of Tooth Shape Design Parameters on the Boundary Size of Nutation Face Gears

The boundary size of a nutation face gear corresponds to its effective tooth width, which further determines its bearing capacity. In this section, the boundary dimensions of a nutation face gear, i.e. the minimum internal radius and the maximum external radius, as well as the change of effective tooth width with the design parameters of the tooth profile are analyzed.

Taking the "face-face" gear pair composed of a fixed face gear and a planetary face gear as an example: based on the basic parameters in Tab. 1, different moduli, pressure angles, cutter teeth numbers and nutation angles are selected as single variables to analyze the influence of single tooth shape design parameters on the boundary size of the nutation face gear.

Tab. 1 Basic parameters of "face-face" gear pair

Modulus m/mm	Tool tooth number N_s	Pressure angle α_0/(°)	Addendum coefficient h_a^*	Teeth number on the fixed side of the planetary face gear N_1	Teeth number of the fixed face gear N_2	Nutation angle β/(°)
3.5	20	20	1.25	63	65	3

2.1 Influence of pressure angle on the boundary dimension of nutation face gears

Pressure angle is a key index to judge transmission performance. In order to analyze the influence of pressure angle on the boundary size of a nutation face gear, taking the pressure angle of reference circle at $\alpha_0=15$, 18, 20, 22, 25, the calculated changing trends of the minimum internal radius, the maximum external radius, and the effective tooth width of the fixed face gear are shown in Fig. 3.

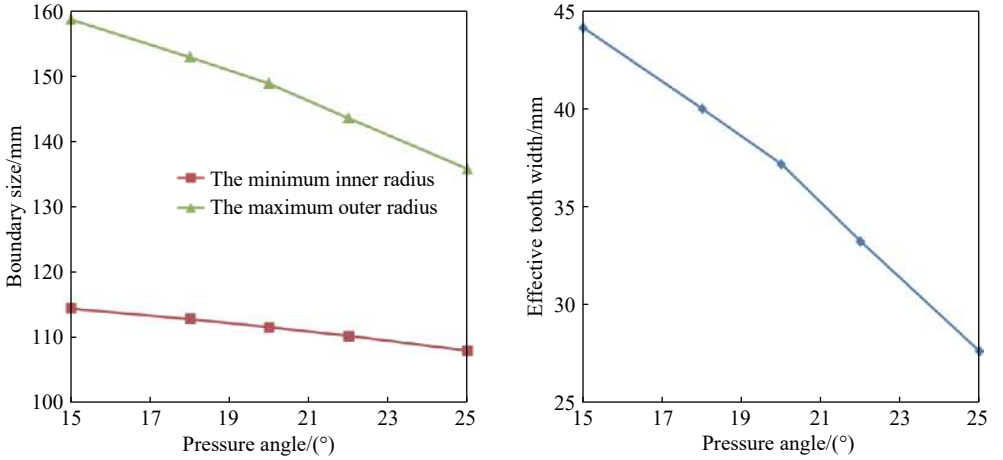

(a) Variation trend of internal and external diameter with pressure angle

(b) Changing trend of the effective tooth width with pressure angle

Fig. 3 Changing trend of the boundary dimension of fixed face gear with pressure angle

It can be seen from Fig. 3 that with the increase of the pressure angle, the minimum internal radius and the maximum external radius of the fixed face gear are gradually reduced. Therefore, for the design of the nutation face gear structure under the given maximum space size, the larger pressure angle can be selected preferentially. However, the effective tooth width of the nutation face gear decreases with the increase of the pressure angle. Therefore, in the design process of the nutation face gear, the pressure angle should be selected reasonably considering the requirements of the structure space and the strength.

2.2 Influence of the cutter teeth number on the boundary size of nutation face gears

The "face-face" gear pair in the nutation face gear is processed by the shaper cutter with the same parameter and the hypothetical cutter. The influence of the cutter teeth number on the boundary dimension of nutation face gear is analyzed. The number of cutter teeth $N_s = 18 - 22$ are taken respectively. The calculated changing trend of the minimum internal radius, the maximum external radius and the limit tooth width of the fixed face gear are shown in Fig. 4.

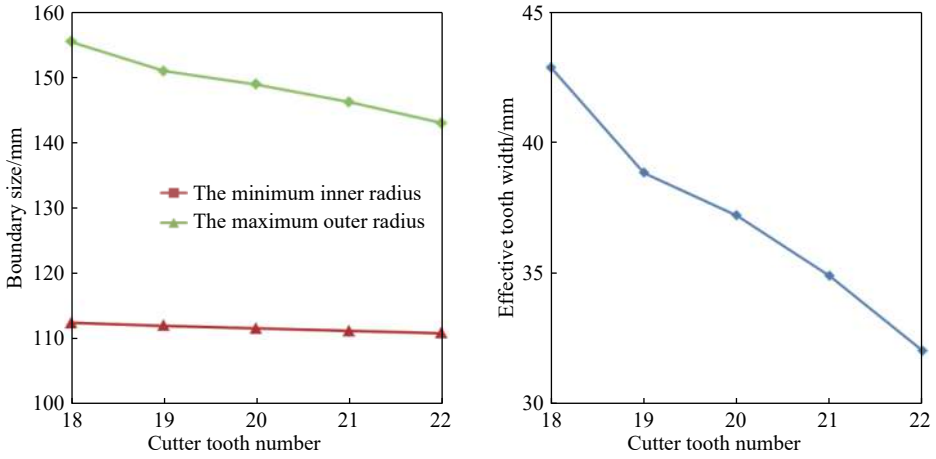

(a) Changing trend of internal and external diameter with the number of cutter teeth

(b) Changing trend of the effective tooth width with the number of cutter teeth

Fig. 4 Changing trend of the boundary dimension of fixed face gear with the number of cutter teeth

It can be seen from Fig. 4 that with the increase of the cutter teeth number, the maximum external radius and the effective tooth width of the nutation face gear decrease gradually, while

the minimum internal radius decreases approximately linearly and the changing trend is not obvious. Therefore, when there are strict requirements on space, a larger number of cutter teeth should be selected if possible; while there are higher requirements on strength, a smaller number of cutter teeth should be selected preferentially.

2.3 Influence of the modulus on the boundary size of nutation face gears

The modulus is a basic parameter to determine gear size. In order to analyze the influence of the cutter modulus on the boundary size of a nutation face gear, the cutter moduli $m = 1 - 5$ are taken respectively. The calculated changing trends of the minimum internal radius, the maximum external radius, and the effective tooth width of the fixed face gear are shown in Fig. 5.

It can be seen from Fig. 5 that with the increase of tool modulus, both the minimum internal radius and the maximum external radius of the nutation face gear increase. In addition, the effective tooth width of the nutation face gear increases linearly with the increase of the modulus when other parameters are constant. This conclusion is of great significance for the spatial petal tooth nutation face gear structure proposed to enlarge the meshing area of gears[20].

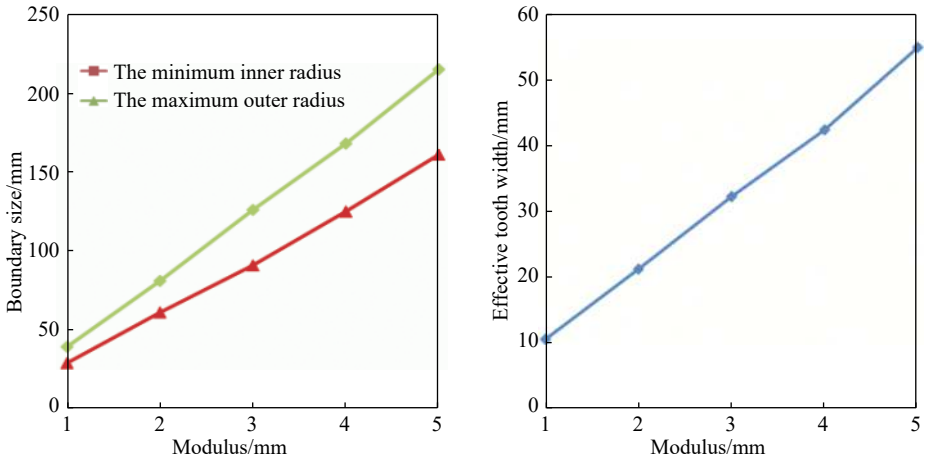

(a) Changing trend of internal and external diameter with the cutter modulus

(b) Changing trend of the effective tooth width with the cutter modulus

Fig. 5 Changing trend of the boundary dimension of fixed face gear with the cutter modulus

2.4 Influence of the nutation angle on the boundary dimension of nutation face gears

The basic principle of nutation face gears is the combination of the nutation motion and the "face-face" gear pair. Therefore, nutation angle is an important design parameter for the nutation face gear. To analyze the influence of the changing nutation angle on the boundary size of nutation face gears, respectively taking nutation angles $\beta = 1^\circ - 6^\circ$, the calculated changing trend of the minimum internal radius, maximum external radius, and the effective tooth width of the fixed face gear are shown in Fig. 6.

It can be seen from Fig. 6 that the minimum internal radius, maximum external radius, and effective tooth width of the nutation face gear decrease with the increase of nutation angle. However, when the nutation angle is between 1° and 2°, the limit size of the gear teeth changes suddenly, and the change tends to be gentle. In the design, if the nutation angle is too small, the space size will be too large. The small change of the nutation angle will have a great influence on the change of axial dimension in the nutation face gear transmission device, especially when the nutation angle is within 5 degrees. With the increase of the nutation angle, the volume and weight of the transmission device will be greatly

reduced. When the nutation angle is more than 5 degrees, the trend is not obvious. Moreover, with the increase of the nutation angle, the bearing load will be increased. At the same time, the additional dynamic load will be more difficult to balance. Therefore, the reasonable range of the nutation angle is $2^\circ - 5^\circ$.

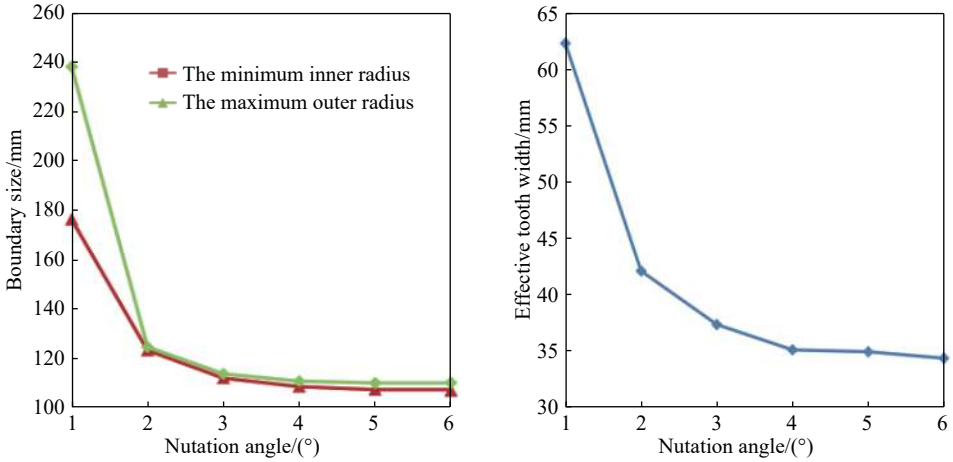

(a) Variation trend of internal and external diameters with nutation angle

(b) Variation trend of the effective tooth width with nutation angle

Fig. 6 Changing trend of the boundary dimension of fixed face gear with nutation angle

3 Conjugate Conditions of the "Face-face" Gear Pair

The conjugate of gear tooth surfaces is based on the concept of envelopes. If the meshing equations of the two gears are equal to that of the cutter, the two gears are conjugate. In the "face-face" gear pair, a pair of meshing gears is formed by cutting tools with the same parameter externally and internally. The equation combining the external face gear and the cutting tool can be written out from Eq. (3) as

$$\begin{aligned} f_1(u_s, \theta_s, \phi_s) =& r_{bs}(1 - m_{s/1}\cos\gamma_{m1}) - \\ & u_s m_{s/1}\sin\gamma_{m1}\cos\phi_\theta = 0 \end{aligned} \tag{12}$$

where $m_{s/1}$ is the ratio of the gear shaper cutter teeth number to the external face gear teeth number.

The meshing equation of the internal face gear and the cutter is

$$\begin{aligned} f_2(u_s, \theta_s, \phi_s) =& r_{bs}(1 - m_{s/2}\cos\gamma_{m2}) - \\ & u_s m_{s/2}\sin\gamma_{m2}\cos\phi_\theta = 0 \end{aligned} \tag{13}$$

where $m_{s/2}$ is the ratio of the gear shaper cutter teeth number to the internal face gear teeth number.

If the internal and external face gears are engaged, it will meet the requirement of the following equation as

$$f_1(u_s, \theta_s, \phi_s) = f_2(u_s, \theta_s, \phi_s) \tag{14}$$

By combining the above formulas, we can get

$$\begin{aligned} f_{fg}(u_s, \theta_s, \phi_s) =& r_{bs}(m_{s/2}\cos\gamma_{m2} - m_{s/1}\cos\gamma_{m1}) + \\ & u_s\cos\phi_\theta(m_{s/2}\sin\gamma_{m2} - m_{s/1}\sin\gamma_{m1}) = 0 \end{aligned} \tag{15}$$

Through the analysis of the boundary dimension of the nutation face gear, the axial parameter u_s of the cutter is limited to

$$\max(u_{s1}^*, u_{s2}^*) \leqslant u_s \leqslant \max(u_{s1}^{**}, u_{s2}^{**}) \tag{16}$$

where the pairs of values u_{s1}^* and u_{s1}^{**}, u_{s2}^* and u_{s2}^{**}, are the minimum and maximum values of the axial parameters of the cutter satisfying the boundary conditions of the external face gear and the internal face gear, respectively, which are determined by the minimum inner radius and the maximum outer radius of the nutation face gear

$$\left.\begin{aligned} u_{s1}^* &= L_{1in}\sin\gamma_{m1} \\ u_{s1}^{**} &= L_{1out}\sin\gamma_{m1} \\ u_{s2}^* &= L_{2in}\sin\gamma_{m2} \\ u_{s2}^{**} &= L_{2out}\sin\gamma_{m2} \end{aligned}\right\} \tag{17}$$

At the same time, the rational angle parameter ϕ_s of the cutter will also meet the following requirements as

$$\max(\phi_{s1}^{*}, \phi_{s2}^{*}) \leqslant \phi_s \leqslant \max(\phi_{s1}^{**}, \phi_{s2}^{**}) \tag{18}$$

where the pairs of values ϕ_{s1}^{*} and ϕ_{s1}^{**}, ϕ_{s2}^{*} and ϕ_{s2}^{**}, are the minimum and maximum values of the cutter angle parameters that meet the boundary conditions of the external and internal face gears, respectively.

According to Eq. (15), the conjugation condition of "face-face" gear pairs can be obtained as

$$\theta_s(u_s, \phi_s) = \cos^{-1}\left[\frac{-r_{bs}(m_{s/2}\cos\gamma_{m2} - m_{s/1}\cos\gamma_{m1})}{u_s(m_{s/2}\sin\gamma_{m2} - m_{s/1}\sin\gamma_{m1})}\right] - (\phi_s + \theta_{s0}) \tag{19}$$

The correctness of the above theoretical derivation has been verified by the analysis of the simulation experiment[20] of the nutation face gear pair and the actual manufacturing of a nutation face gear transmission prototype.

4 Three-Dimensional Modeling of the Nutation Drive with Face Gears

Taking a transmission ratio of 32, input speed of 315.62 r/min, and input power of 45 kW as an example to design a nutation face gear transmission device, the basic parameters of the gear shaper and face gear are calculated and other parameters are shown in Tab. 2. In the table, the nutation angle $\beta = 2.5°$, $i = 1, 2, 3, 4$ represent the fixed face gear, the fixed side of the planetary face gear, the rotating side of the planetary face gear, and the rotating face gear, respectively, and $j = 1, 2$ represent the fixed side and the rotating side, respectively.

Tab. 2 Basic design parameters

Number of face teeth N_i	Tool tooth number N_{sj}	Tool modulus m_j/mm	Tool pressure angle α_{sj}/(°)	Tool pitch angle γ_{sj}/(°)	Pitch angle of gear θ_i/(°)	Angle between shafts γ_i/(°)
31	16	3	25	16.63	33.67	50.31
33					143.82	127.91
33	17	3.5	20	25.30	53.56	78.87
32					123.94	98.63

From Eq. (8), it can be seen that the tooth surface equation of the nutation face gear is an equation with two parameters θ_s and ϕ_s. For the modeling of the nutation face gear, firstly, the pitch cone angle and angle between shafts of each gear are calculated by using the transmission ratio, nutation angle, and other basic parameters, as shown in Tab. 2. Then, the limit size of the nutation face gear is calculated with the undercutting condition and cusp changing condition, and the calculation results are shown in Tab. 3. According to the joint condition of the "face-face" gear pair, the ranges of parameters meeting the conjugating condition are obtained and the calculation results are shown in Tab.4. Then, according to the tooth surface equation of the nutation face gear, the point coordinates of tooth surface are calculated. The generation and three-dimensional modeling of the nutation gear tooth surface can be divided into the following steps.

Tab. 3 Boundary dimension of the nutation face gear

Face gear	The minimum internal radius L_{in} /mm	The maximum external radius L_{out}/mm	Effective tooth width B/mm
Fixed face gear	59.0348	78.7888	19.7540
Fixed side of planetary gear	60.5049	80.3058	19.8009
Rotating side of planetary gear	58.0678	78.6222	20.5546
Rotating face gear	56.9109	77.3829	20.4720

Tab. 4 Parameter range satisfying the conjugate condition

Face to face gear pair	Minimum value of cutter angle parameter $\phi_{s\,min}$/rad	Maximum value of cutter angle parameter $\phi_{s\,max}$/rad	Minimum value of cutter axial parameter $u_{s\,min}$/mm	Maximum value of cutter axial parameter $u_{s\,max}$/mm
Fixed face gear side	–0.5294	–0.4655	75.6517	61.0329
Rotating face gear side	0.2500	0.2769	96.4744	82.0881

① According to the boundary conditions of the nutation face gear and conjugate meshing conditions, the minimum and maximum values of tool angle parameters and axial parameters are obtained.

② Taking n and k discrete values of the equal distance in the range of ϕ_s and u_s, respectively, and letting $\phi_s = C$ (C is a constant), after substituting them into Eq. (19), the relationship equation $\theta_s = f(\phi_s)$ between ϕ_s and θ_s can be derived, and then the corresponding range of θ_s is obtained.

③ By substituting the corresponding values of ϕ_s and θ_s into the tooth surface equations of the internal and external section gears of the "face-face" gear pair, the coordinates of k tooth surface points can be obtained. Different ϕ_s values are selected to get the coordinates of several tooth points, and then are fitted to get the tooth surfaces of the external and internal face gears, respectively, as shown in Fig. 7.

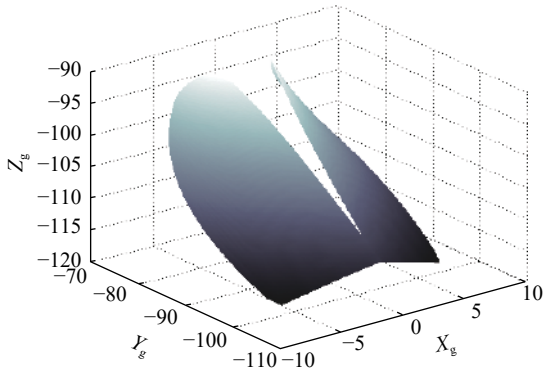

Fig. 7 Boundary dimension of the nutation drive with face gear

④ The calculated coordinates of the tooth surface points are imported into the 3D modeling software, and the 3D model of the tooth is drawn, as shown in Fig. 8. Using the nutation motion principle, the corresponding coordinate system is established, and the single tooth is arrayed to obtain the spatial 3D model of the whole tooth of the nutation face gear.

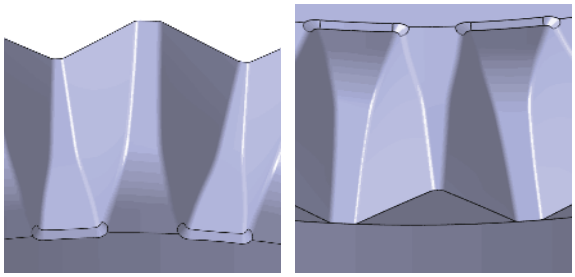

(a) Internal face gear teeth (b) External face gear teeth

Fig. 8 Three-dimensional model of the nutation face gears

⑤ In the same way, the other three gears are modeled, and the assembly is completed according to the motion relationship. Finally, the assembly model of the nutation face gear transmission is obtained as shown in Fig. 9.

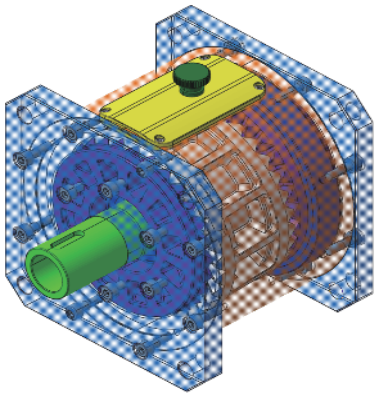

Fig. 9 Three dimensional model of the nutation face gear transmission

5 Conclusion

In this paper, the boundary dimension of a nutation face gear is analyzed in a unified coordinate system. The conditions of no root undercutting and no tip change of the tooth top are obtained. The calculation formula of the boundary dimension of the nutation face gear is derived. It is found that the effective tooth width of

nutation face gears increases linearly with the increase of modulus when other parameters remain unchanged. This conclusion lays a theoretical foundation for proposing a new spatial petal tooth nutation face gear structure. The internal and external radii and effective tooth width of the nutation face gear decrease with the increase of nutation angle, so the reasonable nutation angle range is 2–5 degrees. Based on the meshing principle of spacial gears, the conjugate conditions of the "face-face" gear pair are derived, and the calculation method of discrete points of nutation face gear tooth surfaces is given. The effectiveness of the method is verified by the 3D model of the nutation face gear transmission device.

References:

[1] Wang Guangxin, Deng Jia, Wang Peng, et al. A design method of internal tangent face gear: CN106126844A[P]. 2019-05-14. (in Chinese)

[2] Wang Guangxin, Deng Jia, Wang Peng, et al. Meshing principle and dynamic simulation of nutation drive with face-gear [J]. Journal of Dalian Jiaotong University, 2017, 38(2): 48-54. (in Chinese)

[3] Wang G X, Zhu L L, Wang P, et al. Meshing and bearing analysis of nutation drive with face gear [J]. Recent Patents on Mechanical Engineering, 2020, 13(4): 352-365.

[4] Wang G X, Zhu L L, Wang P. Analysis of tooth stiffness of nutation face gear [J]. Engineering Computations, 2020.DOI:10.1108/ec-11-2019-0522.

[5] Earle B. Analytical mechanics of gear [M]. New York, USA: McGraw-Hill Book Company, 1949.

[6] Litvin F L, Wang J C, Bossler R J, et al. Face-gear drives, design, analysis and testing for helicopter transmission applications [J]. NASA Technical Memorandum, 1992, 10(1): 1-16.

[7] Litvin F L, Fuentes A, Howkins M. Design, generation and TCA of new type of asymmetric face-gear drive with modified geometry [J]. Computer Methods in Applied Mechanics and Engineering, 2001, 43: 5837-5865.

[8] Litvin F L, Fuentes A, Zanzi C, et al. Face-gear drive with spur involute pinion: geometry, generation by a worm, stress analysis [J]. Computer Methods in Applied Mechanics and Engineering, 2002, 191: 2785-2813.

[9] Litvin F L, Fuentes A, Zanzi C, et al. Design, generation, and stress analysis of two versions of geometry of face-gear drives [J]. Mechanism and Machine Theory, 2002, 37(10): 1179-1211.

[10] Litvin F L, Gonzalez-Perez L, Fuentes A, et al. Design, generation and stress analysis of face-gear drive with helical pinion [J]. Computer Methods in Applied Mechanics and Engineering, 2005, 193(36): 3870-3901.

[11] Litvin F L. Gear geometry and applied theory[M]. Shanghai, China: Shanghai Scientific & Technical Publishers, 2008.

[12] Claudio Z, Jose I P. Application of modified geometry of face gear drive [J]. Computer Methods in Applied Mechanics and Engineering, 2005, 194: 3047-3066.

[13] Lu Wenlong, Zhu Rupeng, Zeng Ying. Study on tooth surface curvature for orthogonal face-gear drives [J]. Journal of Nanjing University of Aeronautics & Astronautics, 2000, 32(4): 400-404. (in Chinese)

[14] Yang Lianshun, Zhu Rupeng, Zeng Ying. Analysis of bending stress in perpendicular face gear [J]. Mechanical Science and Technology, 2001, 20(5): 708-709, 713. (in Chinese)

[15] Li Zhengminqing, Zhu Rupeng. Investigation into geometrical design of tooth profile and undercut for orthogonal face gear [J]. Journal of South China University of Technology (Natural Science Edition), 2008, 36(2): 78-82. (in Chinese)

[16] Li Zhengminqing, Zhu Rupeng. Impact of assembly deflection error on contact characteristics of orthogonal face gear drive [J]. Acta Aeronautica Et Astronau Tica Sinica, 2009, 30(7): 1353-1360. (in Chinese)

[17] Chen Hong, Zhu Rupeng, Jing Guanghu. Influence of assembly errors on contact trace of angular bevel face gears [J]. Mechanical Science and Technology, 2011, 30(12): 1990-1994. (in Chinese)

[18] Zschippang H A, Weikert S, Küük K A, et al. Face-gear drive: Geometry generation and tooth contact analysis [J]. Mechanism and Machine Theory, 2019, 142: 1-37.

[19] Zhu L Y, Shi J F, Gou X F. Modeling and dynamics analyzing of a torsional-bending-pendular face-gear drive system considering multi-state engagements [J]. Mechanism and Machine Theory, 2020, 149: 103790.

[20] Li L J, Wang G X, Zhu L L, et al. Configuration design and simulation of novel petal tooth nutation joint drive for robot [C]//Yu H B, Liu J G, Liu L Q, et al. The 12th International Conference on Intelligent Robotics and Applications. Shenyang, China: Springer Verlag, 2019: 652-663.